Recurrence network analysis of multiple local field potential bands from the orofacial portion of primary motor cortex.

Narayan Puthanmadam Subramaniyam[1], Jari Hyttinen[1], *Senior Member, IEEE*,
Nicholas G. Hatsopoulos[2,3], Callum F. Ross[2], and Kazutaka Takahashi[2], *Senior Member, IEEE*

***Abstract*— Local field potentials (LFPs), which have been considered as aggregate signals that reflect activities of a large number of neurons in the cerebral cortex, have been observed to mediate gross functional activities of a relatively small volume of the brain tissues. Historically there have been several frequency bands observed and defined across various brain areas. However, detailed analysis, either spectral analysis or any dynamical analysis of LFPs particularly in the orofacial part of the primary motor cortex (MIo) has not been done before. Here, we recorded LFPs from MIo using an electrode array from a non-human primate during feeding behavior. Then we performed spectral analysis during the whole feeding sequences and to characterize temporal evolution of spectrum around the time of swallow cycles. The spectrogram over the β range showed dynamical change in its power around the swallow cycle onsets. We then characterized dynamical behaviors of LFPs over multiple bands, α, β, low γ, and high γ using two measures from the recurrence network (RN) method, network transitivity, T and average path length L. Temporal profile of T in α and β indicated that there was a sudden change in the dynamical properties around the swallow cycle onsets, while temporal profile of L indicated that a range of -200 to -150 ms and 200ms to the swallow cycle onsets exhibited large changes both in α and β ranges. Therefore, to further understand the involvement of cortical oscillation to behavior, particularly swallowing, the combination of traditional spectral methods and various dynamical methods such as RN method would be essential.**

***Index Terms*— Local field potentials, event evoked potentials, recurrence network, temporal dynamics, motor cortex**

I. Introduction

Cortical rhythms have been studied since early descriptions of oscillations in sensorimotor cortex by Jasper and Penfield [1]. Although our understanding of the underlying circuitry for different bands of oscillations has increased over the years [2], we still know little about the inherent dynamics of each of the oscillation bands and their relation to behaviors. In particular, local field potentials (LFPs) and electroencephalograms (EEG) in the β frequency range (15-30 Hz) are ubiquitous in the primary motor cortex (MI) of mammals including monkeys and humans. The dynamics of the β oscillation has been grossly characterized, based on a temporal profile of the amplitude of the oscillations, such as event related synchronization (ERS) and event related desynchronization (ERD) [3], [4], and phase locking to the instruction cues [5]. However, the dynamical properties of β oscillations have not been well characterized. Recently, it has been reported that phase of β oscillations propagated as plane waves along the rostrocaudal axis of the arm portion of MI during motor preparation and execution for upper arm movement, and are believed to subserve cortical information transfer [6].

However, even in the same MI, the spectral properties of LFPs in the orofacial portion of MI have not been well characterized. It has been showed [7] that prior to volitional swallowing, there is some dynamical behavior in β range based on MEG recording. Furthermore, our recent preliminary study showed [8] that functional connection topology of spiking neurons recorded from the orofacial part of MI is drastically different between during rhythmic chewing cycles and transition from rhythmic chew to swallow cycles. Thus we speculate that there should be some signature of change in β oscillation prior to swallow cycles.

The dynamics of neural activities in general can be considered as nonlinear, mainly arising from the threshold and saturation phenomena [9]. It has been recently shown that methods based on recurrence plots, particularly recurrence networks (RN) can be used to study the structural complexity of the EEG signals [10], [11], [12]. One particular advantage of RN based analysis is that it can be applied to short segments of data, since the network properties like the network transitivity T [13], which is related to the clustering and non-stationarity property of a network [14] or average path length L can still be reliably estimated. The topological characterization of the RN using such network properties can provide insights into the complexity of the dynamics associated with the time series [15].

Therefore, we first used spectral methods to identify any particular power concentrated on certain bands and temporal power variations. Then we used RN method to characterize inherent dynamics of four bands of LFPs, up to α (1- 10 Hz), β (10-30 Hz), low γ (30-80 Hz), and high γ (80-200 Hz) using T and L around the time of swallow cycle onsets.

II. Method

A. Behavior task and data collection

All of the surgical and behavior procedures were approved by the University of Chicago IACUC and conform to the principles outlined in the Guide for the Care and Use of Laboratory Animals (NIH publication no 86-23, revised 1985). One female macaque monkey was trained to feed with her right hand while restrained in a primate chair. Her head was restrained with a halo coupled to the cranium through chronically implanted headposts. At least one month prior to data recording, three 0.5 mm diameter tantalum balls (RSA Biomedical, Sweden) were implanted by hypodermic needle into the anterior, middle, and posterior regions of the tongue at midline, under isoflurane anesthesia. Post-surgery, the monkey was trained to perform a manual feeding task and ate various types of foods in preparation for videofluoroscopy (VF). While the monkey self-fed various foods, two-dimensional lateral view VF of jaw and tongue movements were acquired at a frame rate of 100 Hz using an OEC 9600 C-arm fluoroscope retrofitted with a Redlake Motion Pro 500 video camera (Redlake MASD LLC, San Diego,

[1]N.P.S. and J.H. are with Department of Elecronics and Communications Engineering, Tampere University of Technology. (Email: {narayan.ps, jari.hyttinen}@tut.fi).

[2]N.G.H. C.F.R. and K.T. are with the Department of Organismal Biology and Anatomy, University of Chicago, IL 60637, USA (Email: {nicho, rossc, kazutaka}@uchicago.edu). This work was supported by NIH R01 DE023816 and R01 NS04853.

[3]N.G.H. is with the Committee on Computational Neuroscience, University of Chicago, Chicago, IL 60637, USA.

CA, USA) [16]. Detailed methods of collecting jaw kinematic data are described elsewhere [17], [18]. Three dimensional jaw kinematic data were collected in the coordinate system of the cranium using an infrared light video-based motion analysis system (Vicon Motion Tracking System with 10 MX40 cameras with sampling rate of 250 Hz) which tracked reflective markers coupled to the mandible and cranium using bone screws. The marker coordinates were bi-directionally lowpass filtered with a 4th order Butterworth filter with 15 Hz cutoff frequency. Using movements of the mandibular marker, jaw movement cycles were defined by two consecutive maximum gapes (i.e., maximum open). By checking the behavior with VF data, we identified swallow cycles and focused on time windows ± 400 ms around the beginning of swallow cycles in the current study.

We recorded LFPs from a chronically implanted 100-electrode Utah microelectrode array (1.5 mm in length, 10 x 10 grid, 400 μm interelectrode spacing, Blackrock Microsystems, Utah, USA,) in the orofacial area of primary motor cortex (MIo) on the left side of the monkey. LFPs from up to 96 channels were recorded at 1 kHz. The LFP data for each channel were filtered over α (3-10 Hz), β (10-30 Hz), low γ (30-80 Hz), and high γ (80-200 Hz) respectively first, then were chunked into [-600, 599] ms centered on the maximum gape (or the beginning) of swallow cycles (74 events), then a sliding window of 400 ms with a 1 ms increment was used to perform RN analysis over [-400,400] ms centered on the beginning of swallow cycles.

III. Recurrence Network Analysis

Recurrences are a fundamental property of many dynamical processes and the method of recurrence plots (RPs) can be used to visualize recurrences in the phase space [19]. Given a scalar time series $y(t) = \{y_1, y_2, \cdots, y_N\}$, one can reconstruct an m-dimensional phase space vector $\mathbf{y}_i = \left(y_i, y_{i+\tau}, \cdots, y_{i+(m-1)\tau}\right)$ by choosing a suitable embedding dimension m and lag τ [20]. A recurrence matrix can be given as

$$R_\varepsilon(i,j) = \Theta(\varepsilon - ||\mathbf{y}_i - \mathbf{y}_j||), \tag{1}$$

where $\mathbf{y}_i$ and $\mathbf{y}_j$ are state vectors at time $t = t_i$ and t_j respectively, Θ is the Heaviside function, $||\cdot||$ is the distance norm (manhattan or euclidean or maximum) and ε is the recurrence threshold, which is basically the phase space distance. The recurrence matrix $\mathbf{R}_\varepsilon$ can be further reinterpreted as an adjacency matrix of a complex network using the following transformation [15], [21]

$$A_\varepsilon(i,j) = R_\varepsilon(i,j) - \delta(i,j), \tag{2}$$

where $\delta(i,j)$ is the Kronecker delta to make the elements along the diagonal of the adjacency matrix $\mathbf{A}$ zero. The adjacency matrix $\mathbf{A}_\varepsilon$ represents a complex network known as the ε-recurrence network (RN). Also, the adjacency matrix $\mathbf{A}_\varepsilon$ preserves the symmetric properties of the recurrence matrix $\mathbf{R}_\varepsilon$ and thus the ε-recurrence network represents a simple graph [22]. Using graph theoretical measures, one can now characterize the structural properties of the underlying dynamical system represented by the univariate time series $y(t)$. The toolbox of complex network theory offers a repository of large measures. In this work, we look at two global measures, the network transitivity T [13], which is related to the clustering property of a network [14] and is given as,

$$T = \frac{\sum_{i,j,k=1}^{N} A(i,j)A(j,k)A(k,i)}{\sum_{i,j,k=1}^{N} A(i,j)A(k,i)}, \tag{3}$$

and the average path length L [13] given as,

$$L = \frac{1}{N(N-1)} \sum_{i \neq j} d(i,j), \tag{4}$$

where $d(i,j)$ is the geodesic distance between two vertices in a network and N is the number of vertices. The network transitivity for a RN characterizes the global dimensionality of a system [23]. Dynamical systems exhibiting periodic dynamics display high values for T and L compared to systems exhibiting chaotic dynamics. Thus, these measures give an insight into the regularity of the underlying dynamics.

By dividing a time series into small windows, moving window recurrence network analysis can be performed to obtain a time-varying profile of these network measures. Using such an approach, one can identify dynamical transitions in a time series. Particularly, measures like T and L are sensitive to dynamical transitions in a complex system as demonstrated by their application to paleo-climate [24] and biogeoscience data [25]. In order to obtain the embedding parameters τ and m, we used the first local minima of the auto-mutual information and the modified false nearest neighbor method respectively [20]. For most of the data, we observed that m varied between 3 and 5. As a trade off between data length (400 samples) and embedding dimension, we settled for $m = 3$ for all the windows. τ varied between 30 and 2 for bands ranging between α and high γ. Additionally, we set the recurrence rate RR to a suitable choice of 0.05 [24].

IV. Results

A. Spectral profiles of LFPs

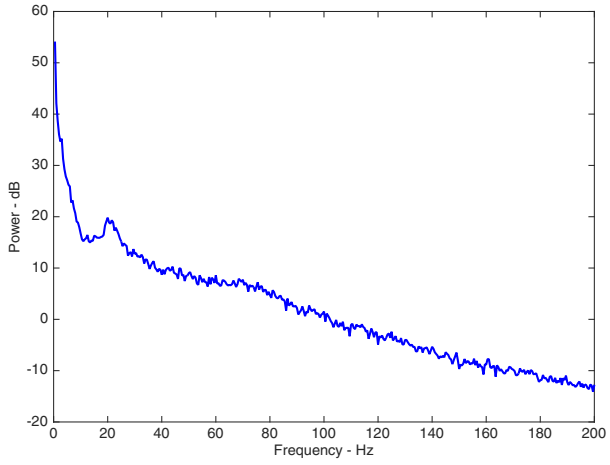

Fig. 1. Averaged power spectrum of LFP computed over all channels recorded by MIo array. There is a clear peak around 20Hz in this subject over β range and a small and wide peak in a low γ range. Harmonics of 60Hz noise was removed by a set of notch filters.

First, Fig. 1 shows a power spectrum of LFPs computed over all feeding sequences across all channels. The multi-taper method from Chronux (http://chronux.org/) [26] was used and the parameters used were: $[TW, K] = [3, 5]$, where TW denoted the time-bandwidth product and K being the number of tapers. There were a distinct peak around 18-19 Hz over the β oscillation and a small peak around 40Hz over the low γ range. Harmonics of 60Hz line noise was notched out for the further analysis.

Fig. 2 showed a set of spectrograms of LFPs computed for 4 bands over $[-700, 700]$ ms of all swallow cycle onsets. The parameters used for the multi-taper method were the same as

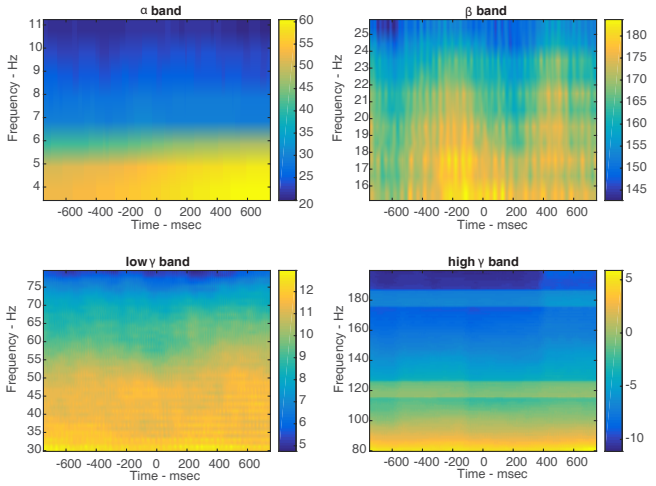

Fig. 2. Spectrograms of 4 speficied bands of LFP, α, β, low γ and high γ ranges.

above and a moving window of 500 ms with a 1 ms increment was used. There was a power increase in δ-θ boundary 200-300 ms after swallow cycle onset. The β range showed dynamical behavior starting with low power and peaks about -200 ms and kept attenuating and a weak increase again after 200 ms from the onset. Neither low or high γ ranges show significant modulations around the swallow cycle onsets.

B. Temporal profiles of Network transitivity T and Average path length L across different bands

The mean network transitivity T for evoked responses across all channel for the four different frequency bands were shown in Fig. 3. The α and β bands showed somewhat similar temporal profiles where sharp drops of T around or slightly before 0 ms and rebounding were observed. While the low γ band somewhat monotonically decreased its T valuesm the high γ band exhibited a brief decrease around 200 ms.

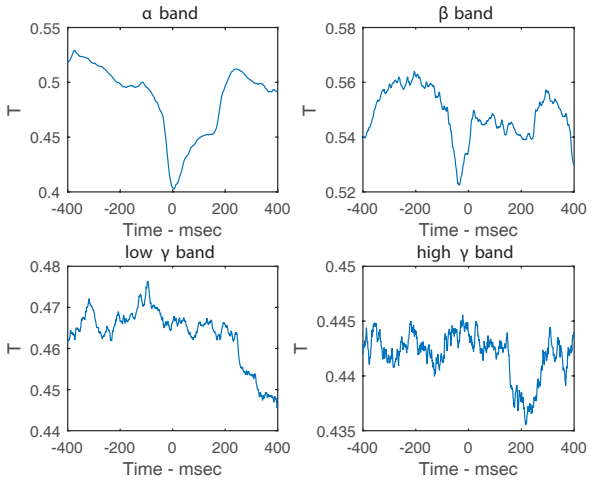

Fig. 3. Network transitivity T for the four bands of LFPs.

The mean average path lenghts L for evoked responses across all channels for the four different frequency bands were shown in Fig. 4. Unlike the network transitivity measure T, the values of the average path length L was inversely proportional to the frequency bands. For L, the α and β bands were not sharing similar profiles in comparison to T. The α band exhibited a small variation until a local minima around -100 ms, then a sudden increase up to 0 ms, then a decay. On the other hand, the β band showed somewhat constant values of L except for around -200 ms. The low γ band did not show significant modulation in its spectrogram, but the path length showed a dynamical behavior where a sudden drop in L took place around -175 to -150 ms followed by a monotonic increase. The high γ showed a local maxima at around -130 ms followed by a decrease up to around -15 ms.

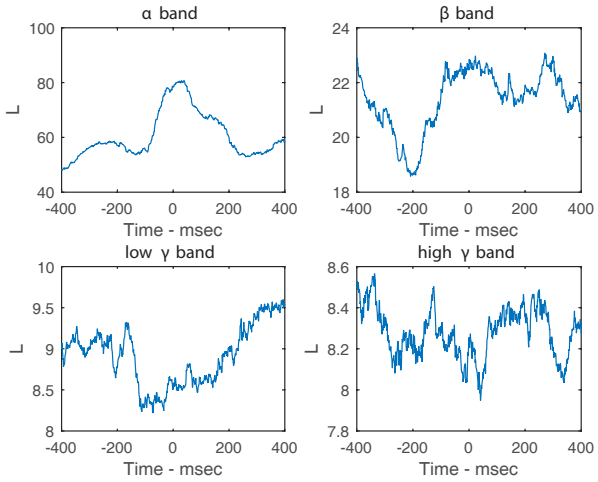

Fig. 4. Average path length L across the four bands of LFPs.

V. Discussions

We characterized the evoked responses of intracortically recorded LFPs from MIo across the four bands α, β, low γ, and high γ. The β band showed some modulations in terms of its power profile against swallow cycle onsets, not EMG onsets as in [7]. Thus, our simple spectral analysis further suggests that the β range in MIo is a band of interest to establish relation between swallowing and LFPs. Our new RN method shed a light to exhibit that potentially other bands could be related to swallowing behavior. The network transitivity, T, of the α and β bands showed comparable temporal profiles, sharp drop of T values start before 0 ms, while the temporal evolution of power themselves have any similar relation. It is not clearly definitive, based on this preliminary study, that this sharp drop prior to 0 ms in both α and β is a signature of swallowing, however, this will be a hypothesis to be tested in our future study with data from more animals.

Based on the analysis of average path length, L, the α and the β bands show dissimilar temporal evolutions especially at the times of their local minima, -175 ms and -200 ms respectively. Thus, those reduction in L on both bands may indicate a timing similar to what we commonly observe as ERD in β oscillation around movement onset for visuomotor task with upper limb. Although swallowing is not a visuomotor behavior, the cortical β activity decreases its periodic or synchronized oscillatory activities across the entire recording area from MIo. The behavioral relevance of this decrease is clearly unknown, but this may reflect a decision of a swallow reflected in the cortex. Furthermore, another set of local minima around 200 ms and $150-200$ ms for those two bands is happening right around the time that actual swallowing activity takes place (data not shown). Thus a decrease in L to reach to

those local minima may indicate another type of an important event such as kinematic coordination of tongue, jaw, and other oropharyngeal components involved in swallowing or change in cortical-subcortical interactions such that "noisy" cortical activity would not affect semi-automatic reflex movement, swallowing, controlled by the brainstem swallow center. Although these dynamical measures are not computable in real time, they guide us as to which time window we need to look at in relevant neural, kinematics, or kinetic signals. Furthermore, if we can predict the sudden changes in L that we found based on the evoked responses, then we can potentially use LFPs over α or β bands to predict swallowing events for brain machine interface for dysphagia patients.

In our current study, we only looked at evoked movements locked to swallow cycle onsets across all channels. However, we are in the process to expand this analysis to single trials as well as to develop statistical assessment of peaks in various network measures not limited to T and L used in this study. Furthermore, the variability of those network measures in different channels has to be studied. Our array spans 4x4 mm in the orofacial cortex, but as it has been shown [27] that local responses characterized by intracortical microstimulation (ICMS) are fairly heterogeneous. Therefore, we need to incorporate either functional or spatial interactions of these measures from all the channels from our arrays to further advance our understanding of cortical LFP dynamics and its relation to swallowing or other orofacial behaviors.

VI. Acknowledgement

The authors would like to thank members of Hatsopoulos laboratory at University of Chicago for surgery, training, and data collection from the monkey and discussions. This work was completed in part with resources provided by the University of Chicago Research Computing Center (RCC).

References

[1] H. Jasper and W. Penfield, "Electrocorticograms in man: Effect of voluntary movement upon the electrical activity of the precentral gyrus," *Archiv fr Psychiatrie und Nervenkrankheiten*, vol. 183, no. 1-2, pp. 163–174, 1949.

[2] T. Womelsdorf, T. A Valiante, N. T Sahin, K. J. Miller, and P. Tiesinga, "Dynamic circuit motifs underlying rhythmic gain control, gating and integration.," *Nature neuroscience*, vol. 17, no. 8, pp. 1031–9, Aug. 2014.

[3] C. Neuper and G. Pfurtscheller, "Event-related dynamics of cortical rhythms: frequency-specific features and functional correlates," *International Journal of Psychophysiology*, vol. 43, no. 1, pp. 41 – 58, 2001, Thalamo-Cortical Relationships.

[4] M.T. Jurkiewicz, W.C. Gaetz, A.C. Bostan, and D. Cheyne, "Post-movement beta rebound is generated in motor cortex: Evidence from neuromagnetic recordings," *NeuroImage*, vol. 32, no. 3, pp. 1281 – 1289, 2006.

[5] A Reimer, P Hubka, A K Engel, and A Kral, "Fast propagating waves within the rodent auditory cortex," *Cereb Cortex*, vol. 21, pp. 166–177, 2011.

[6] D. Rubino, K. A. Robbins, and N. G. Hatsopoulos, "Propagating waves mediate information transfer in the motor cortex.," *Nature Neuroscience.*, vol. 9, no. 12, pp. 1549–1557, Dec. 2006.

[7] I. K. Teismann, R. Dziewas, O. Steinstraeter, and C. Pantev, "Time-dependent hemispheric shift of the cortical control of volitional swallowing," *Human brain mapping*, vol. 30, no. 1, pp. 92–100, 2009.

[8] K. Takahashi, L. Pesce, J. Iriarte-Diaz, M. Best, S. Kim, T.P. Coleman, N.G. Hatsopoulos, and C.F. Ross, "Granger causality analysis of state dependent functional connectivity of neurons in orofacial motor cortex during chewing and swallowing," in *Soft Computing and Intelligent Systems (SCIS) and 13th International Symposium on Advanced Intelligent Systems (ISIS), Joint 6th International Conference on*, Nov 2012, pp. 1067–1071.

[9] R. G. Andrzejak, K. Lehnertz, F. Mormann, C. Rieke, P. David, and C. E. Elger, "Indications of nonlinear deterministic and finite-dimensional structures in time series of brain electrical activity: Dependence on recording region and brain state," *Physical Review E*, vol. 64, no. 6, pp. 061907, 2001.

[10] N. P. Subramaniyam and J. Hyttinen, "Characterization of dynamical systems under noise using recurrence networks: Application to simulated and eeg data," *Physics Letters A*, vol. 378, no. 46, pp. 3464 – 3474, 2014.

[11] N. P. Subramaniyam and J. Hyttinen, "Analysis of nonlinear dynamics of healthy and epileptic eeg signals using recurrence based complex network approach," in *Neural Engineering (NER), 2013 6th International IEEE/EMBS Conference on*. IEEE, 2013, pp. 605–608.

[12] N. P. Subramaniyam and J. Hyttinen, "Dynamics of intracranial electroencephalographic recordings from epilepsy patients using univariate and bivariate recurrence networks," *Physical Review E*, vol. 91, no. 2, pp. 022927, 2015.

[13] S. Boccaletti, V. Latora, Y. Moreno, M. Chavez, and D.U. Hwang, "Complex networks: Structure and dynamics," *Physics reports*, vol. 424, no. 4, pp. 175–308, 2006.

[14] A. Barrat and M. Weigt, "On the properties of small-world network models," *The European Physical Journal B-Condensed Matter and Complex Systems*, vol. 13, no. 3, pp. 547–560, 2000.

[15] R.V. Donner, Y. Zou, J. F. Donges, N. Marwan, and J. Kurths, "Recurrence networksa novel paradigm for nonlinear time series analysis," *New Journal of Physics*, vol. 12, no. 3, pp. 033025, 2010.

[16] C. F. Ross, A. L. Baden, J. Georgi, A. Herrel, K. A. Metzger, D. A. Reed, V. Schaerlaeken, and M. S. Wolff, "Chewing variation in lepidosaurs and primates," *The Journal of Experimental Biology*, vol. 213, no. 4, pp. 572–584, 2010.

[17] D. A. Reed and C. F. Ross, "The influence of food material properties on jaw kinematics in the primate, cebus," *Arch Oral Biol.*, vol. 55, no. 12, pp. 946 – 962, 2010.

[18] J. Iriarte-Díaz, D. A. Reed, and C. F. Ross, "Sources of variance in temporal and spatial aspects of jaw kinematics in two species of primates feeding on foods of different properties," *Integr Comp Biol.*, vol. 51, no. 2, pp. 307–319, 2011.

[19] N. Marwan, M. C. Romano, M. Thiel, and J. Kurths, "Recurrence plots for the analysis of complex systems," *Physics Reports*, vol. 438, no. 5, pp. 237–329, 2007.

[20] H. Kantz and T. Schreiber, *Nonlinear time series analysis*, vol. 7, Cambridge university press, 2004.

[21] N. Marwan, J. F. Donges, Y. Zou, R. V. Donner, and J. Kurths, "Complex network approach for recurrence analysis of time series," *Physics Letters A*, vol. 373, no. 46, pp. 4246–4254, 2009.

[22] R. V. Donner, J. F. Donges, Y. Zou, and J. H. Feldhoff, "Complex network analysis of recurrences," in *Recurrence Quantification Analysis*, pp. 101–163. Springer, 2015.

[23] R. V. Donner, J. Heitzig, J. F. Donges, Y. Zou, N. Marwan, and J. Kurths, "The geometry of chaotic dynamicsa complex network perspective," *The European Physical Journal B-Condensed Matter and Complex Systems*, vol. 84, no. 4, pp. 653–672, 2011.

[24] R. V Donner, M. Small, J. F. Donges, N. Marwan, Y. Zou, R. Xiang, and J. Kurths, "Recurrence-based time series analysis by means of complex network methods," *International Journal of Bifurcation and Chaos*, vol. 21, no. 04, pp. 1019–1046, 2011.

[25] H. Lange and S. Boese, "Recurrence quantification and recurrence network analysis of global photosynthetic activity," in *Recurrence Quantification Analysis*, pp. 349–374. Springer, 2015.

[26] P. Mitra and H. Bokil, *Observed Brain Dynamics*, Oxford University Press, New York, 2008.

[27] N. Hatanaka, H. Tokuno, A. Nambu, T. Inoue, and M. Takada, "Input-output organization of jaw movement-related areas in monkey frontal cortex," *Journal of Comparative Neurology*, vol. 492, no. 4, pp. 401–425, 2005.